

# Dr H Similarity

*by Saif Althagafi*

---

**Submission date:** 21-Dec-2022 01:17PM (UTC+0000)

**Submission ID:** 147946089

**File name:** .pdf (485.28K)

**Word count:** 3760

**Character count:** 20289

**Highly efficient of green synthesis of nanostructured ZnFe<sub>2</sub>O<sub>4</sub> photocatalysts by using *Ziziphus mauritiana* and *Salvadora persica* extracts for photocatalytic degradation of crystal violet under sunlight**

11

Hossein Bayahia\*

Chemistry Department, Faculty of Science, Albaha University,  
Albaha, Saudi Arabia

\*Correspondence author

E-mail address: [hbayahia@bu.edu.sa](mailto:hbayahia@bu.edu.sa) (H. Bayahia).

**Abstract:** The current study is aimed to investigate the photocatalytic degradation of crystal violet dyes solution in the presence of modified ZnFe<sub>2</sub>O<sub>4</sub> photocatalysts by *Ziziphus mauritiana* and *Salvadora persica* extracts in sunlight. Regardless of the extracts used, the modified ZnFe<sub>2</sub>O<sub>4</sub> catalysts demonstrated excellent photocatalytic degradation. However, the catalysts modified using *Salvadora persica* extract achieved superior photocatalytic degradation of crystal violet dye. ZnFe<sub>2</sub>O<sub>4</sub> with *Salvadora persica* yielded smaller particles with a larger surface area, smaller band gap energy and a better distribution of differently sized particles than by using *Ziziphus mauritiana*. This photocatalyst also demonstrated stability, being able to be reused at least five times with minimal loss of catalytic ability, falling from 91% at the first iteration to 85% by the fifth reuse. These materials were prepared easily using an environmentally friendly method.

**Keywords:** ZnFe<sub>2</sub>O<sub>4</sub>, *Extracts*, degradation, crystal violet, sunlight.

## 1. Introduction

Today, the water contamination and the energy crisis are the major concerns and they lie in the remarkable processes of photocatalysis. The methods of synthesis of nanoparticles along with the photocatalytic degradation strategy have been broadly used to eliminate of harmful industrial pollutants and colour in the wastewater by elimination of recombination of electron and hole to their utilization

in the photocatalytic degradation and water splitting reactions . One is the most important and promising development is green synthesis, as it enables the creation of photocatalysts, antibacterial compounds and biofuels in a manner that is non-toxic and environmentally friendly, using water as the solvent and compounds extracted from leaves. Furthermore, these methods of synthesis require lower pressures and temperatures than traditional synthesis methods.

For example, by using leaf extracts obtained from various plant species,  $M^{2+}Fe_2O_4$  nanoparticles can be prepared, where  $M^{2+}$  can represent gold (Au), cobalt (Co), nickel (Ni), copper (Cu), or silver (Ag) among other metals.

Using zinc to create  $ZnFe_2O_4$  catalysts is attractive, as these nanoparticles are highly magnetic and electrically stable. Furthermore they have biomedical properties, can be prepared using diverse methods and come in a range of sizes, shapes and purities. These qualities lend these materials to be used in a broad range of applications.

To improve the activity of  $ZnFe_2O_4$  photocatalysts, different types of plant extract were used such as *Indigofera tinctoria* and *Iresine herbstii*. The products were calcined at different calcination temperatures, and the increasing of calcination temperatures led to reduce the particle sizes and their photodegradation performances of dyes were increased in sunlight. The extracts were acted as both chelating and reducing agents, yielding products with high catalytic activity, pure phases and good crystallinity and size dispersion. The product also showed good

voltammetric responses, having a high <sup>5</sup> electrochemical performance, making it a promising material for use in electrochemical applications.

Drawing upon the research described in and building upon our earlier work ZnFe<sub>2</sub>O<sub>4</sub> was prepared and calcined using 500–900°C. Maximal dye degradation was achieved 600°C. In the current study, ZnFe<sub>2</sub>O<sub>4</sub> that had been calcined at 600°C was modified using leaf extracts from *Ziziphus mauritiana* and *Salvadora persica*. The materials were characterized and their activities were investigated in the degradation of CV dye. The findings in this work reveal that the performance of these bionanomaterials is more efficient than that of other nanomaterials modified by plant extracts.

## <sup>12</sup> 2 Experimental

### 2.1 Materials and methods

All chemicals were of analytical grade and used in the state as purchased, and did not undergo addition or modification. p-Toluenesulfonic acid (C<sub>7</sub>H<sub>8</sub>O<sub>3</sub>S.H<sub>2</sub>O) was purchased from LOBA CHEMIE PVT.LTD, whilst Fe(NO<sub>3</sub>)<sub>3</sub>.9H<sub>2</sub>O, <sup>17</sup> Zn(NO<sub>3</sub>)<sub>2</sub>.6H<sub>2</sub>O and NaOH were obtained from Sigma-Aldrich. *Ziziphus mauritiana* and *Salvadora persica* leaves were collected from the Albaha region of Saudi Arabia. The CV dye was purchased from BHD.

### 2.2 Preparation of *Ziziphus mauritiana* and *Salvadora persica* leaf extracts

Fresh and healthy leaves were rinsed in distilled water then left to dry for 7–10 days at room temperature. Once dry, 10 g of leaves was immersed in 100 ml of 65°C distilled water and left to infuse for 1 h. The infusion was cooled to room temperature then it was filtered to remove the leaves, which were discarded and used to prepare the ZnFe<sub>2</sub>O<sub>4</sub> photocatalysts.

### 2.3 Preparation of ZnFe<sub>2</sub>O<sub>4</sub> using leaf extracts

Appropriate quantities of Zn(NO<sub>3</sub>)<sub>2</sub>·6H<sub>2</sub>O and Fe(NO<sub>3</sub>)<sub>3</sub>·9H<sub>2</sub>O were weighed out then added to the plant extract solution. The solution was stirred until the temperature reached 65°C, whereupon 1 g of C<sub>7</sub>H<sub>8</sub>O<sub>3</sub>S·H<sub>2</sub>O was added, and stirred continuously for 1 hr; the temperature was kept constant at 65°C. Co-precipitation was instigated by adding 1 M of NaOH solution in a dropwise manner until pH 12. The precipitate was retrieved, filtered and rinsed in distilled water before rinsing once in ethanol. The solids were dried overnight at 120°C then annealed at 600°C for 24 h.

### 2.4 Characterisation techniques

FT-IR Spectrometry (PerkinElmer Spectrum 100) was conducted using the KBr pellet method, in the range of 400-4000 cm<sup>-1</sup>. X-ray diffraction analysis was performed using a Bruker D8 advanced powder diffractometer instrument; the diffractometer used Cu K<sub>α</sub> radiation ( $\lambda = 1.5416 \text{ \AA}$ ) at the 0.2 $\theta$  scale, in the range of 10°–80°, with a scanning step of 0.2° at 45kV and 40mV. Scanning electron

microscopy (SEM) analysis was conducted using a Hitachi S-4800 device (Tokyo, Japan). Also, a JEOL (JEM-2100F) transmission electron microscope (TEM) was used. A UV-vis spectrophotometer (Philips 8800).

### 2.5 Photocatalytic reactions

CV dye solution was using batch reactor at neutral media and under sunlight. 15 mg of photocatalyst was added to 20 mL. The mixture was kept in darkness for 30 min to reach the equilibrium. Then the mixture was exposed to sunlight. Repeated reactions were conducted every five minutes until all the dye had completely degraded. Then the separated and clear solution was analysed using UV-vis spectroscopy. Equation (1) was used to calculate the percentage of degradation.

$$\text{Degradation (\%)} = \frac{A_0 - A_t}{A_0} \times 100. \quad (1)$$

Where,  $A_0$  is the initial absorbance of dye and  $A_t$  is the absorbance of the dye at a different time of the reaction.

## 3 Results and discussion

### 3.1 FT-IR analysis

FT-IR was used to identify the functional groups that contributed to the reduction and stabilisation of the synthesized photocatalytic materials. Figure 1 shows the IR spectra for *Salvadora persica* and *Ziziphus mauritiana* extracts to be in the range of 500-4000  $\text{cm}^{-1}$ , it also shows the spectra for the extract-modified  $\text{ZnFe}_2\text{O}_4$

nanoparticles. The peaks reflect the OH, C-O, CH and C=O functional groups. *Salvadora persica* presents broad peaks of free O-H at 3400, C-H at 2369, the bands at 1632 and 1063  $\text{cm}^{-1}$  donate the C=O and C-O respectively and stretching vibrations of C-H at 1439  $\text{cm}^{-1}$ .

The spectra of modified  $\text{ZnFe}_2\text{O}_4$  show peaks that reflect C-H stretch at 2915  $\text{cm}^{-1}$  and C=O stretching band at 1063  $\text{cm}^{-1}$ . A broad peak at 3440  $\text{cm}^{-1}$  is attributed to the stretching vibrations of O-H bonded and  $-\text{NH}_2$  functional groups. Meanwhile, the band at 400-850  $\text{cm}^{-1}$  is assigned to M-O stretching vibrations.

These results indicate that the extract contains phytochemicals such as alkaloids, flavonoids, glycosides, tannins and phenolics. These functional groups are reported on  $\text{ZnFe}_2\text{O}_4$ , which facilitates the particles' photocatalytic activity. These functional groups are reported on  $\text{ZnFe}_2\text{O}_4$ , which facilitates the particles' photocatalytic activity. These results are consistent with those published elsewhere.

Figure 1. FT-IR spectra of (a) *Salvadora persica* extract; (b)  $\text{ZnFe}_2\text{O}_4$  modified by *Salvadora persica* extract; (c) *Ziziphus mauritiana* extract; (d)  $\text{ZnFe}_2\text{O}_4$  modified by *Ziziphus mauritiana* extract.

### 24 3.2 XRD analysis



Figure 2 presents the XRD results of modified and pure ZnFe<sub>2</sub>O<sub>4</sub> photocatalyst. Pure ZnFe<sub>2</sub>O<sub>4</sub> has a crystalline structure and sharp XRD peaks and modifying ZnFe<sub>2</sub>O<sub>4</sub> with plant extracts reduced the crystallinity of ZnFe<sub>2</sub>O<sub>4</sub>. This can be explained by carbon annealing at 600°C, resulting in an amorphous structure. The diffraction patterns at 30.14, 35.54, 36.53, 43.15, 53.41, 56.93 and 62.35, which are indexed to (2 2 0), (3 1 1), (2 2 2), (4 0 0), (4 2 2), (5 1 1) and (4 4 0) lattice planes indicate that pure ZnFe<sub>2</sub>O<sub>4</sub> nanostructures have a face-centred cubic structure. The assigned diffraction lines are in excellent agreement with corresponding JCPDS No: 00-022-1012. The peaks at 22.91 and 24.09, which are assigned to Fe<sub>2</sub>O<sub>3</sub> impurities that exhibited in the structure of ZnFe<sub>2</sub>O<sub>4</sub> treated by *Ziziphus mauritiana* extract. The observed pattern of ZnFe<sub>2</sub>O<sub>4</sub> and Fe<sub>2</sub>O<sub>3</sub> are consistent with JCPDS cards of # 22-1012 and #87-1166 respectively.

On the basis of the half-width of the 3 1 1 reflection in the powder pattern, the average grain size, which was calculated using the Debye-Scherrer formula:  $D = 0.9\lambda/\beta \cos \theta$ , where D is the crystalline size,  $\lambda$  is the wavelength (1.54,  $\beta$  is the width of the XRD peak posted at 35.54° at half maximum height (FWHM)) and  $\theta$  is the Bragg diffraction angle. Table 1 presents the XRD results of the nanoparticles crystalline grain sizes.

Figure 2. XRD patterns of pure and modified ZnFe<sub>2</sub>O<sub>4</sub> photocatalysts

Table 1: Data of crystallite, average particle size and band gap

Sample	Position of highest peak (deg.)	Crystalline Size (nm)	Average particle size (nm)	Optical Band Gap energy (eV)
ZnFe <sub>2</sub> O <sub>4</sub> <i>Ziziphus mauritiana</i>	35.49	18.39	7.59	1.37-2.12
ZnFe <sub>2</sub> O <sub>4</sub> <i>Salvadora persica</i>	33.59	17.30	5.95	1.43-1.82

### 3.3 Morphological analysis

#### 3.3.1 SEM and EDS analysis

The results of the SEM analysis of the modified ZnFe<sub>2</sub>O<sub>4</sub> are shown in Figures 3 (a) and (b). This reveals that all of samples have broadly spherical morphologies with numerous agglomerations of flakes. Due to the low magnification of the SEM images, it was difficult to obtain measurements of the size of the particles. Treating the ZnFe<sub>2</sub>O<sub>4</sub> nanoparticles with different plant extracts yielded products that differed in their morphologies. As Figure 3 (a) demonstrates, treating ZnFe<sub>2</sub>O<sub>4</sub> with *Ziziphus mauritiana* extracts produced coarser particles than treating the nanoparticles with *Salvadora persica*, which were finer and more spherical in shape (Figure 3 (b)).

To identify the elemental compositions of the plant-extract modified samples, EDS was used (Figures 3 (c) and (d)). From these images, it can be seen that the samples were pure; the small amount of carbon present was derived from the plant extracts. The EDS results show that Zn, Fe and O were the only elements present in all of the samples. The plant extracts modified a reasonable percentage of the Zn, Fe and

O elements of the  $\text{ZnFe}_2\text{O}_4$ . The other signals are consistent with the absorption of carbon, confirming the presence of plant extract-derived organic compounds, which act as capping ligands for the photocatalysts. The EDS results presented in Figure 3 (c) and (d) are aligned with others reported elsewhere.

Figure 3. Figure 3. SEM images of  $\text{ZnFe}_2\text{O}_4$  modified with (a) *Ziziphus mauritiana* (b) *Salvadora persica*; and EDS images of  $\text{ZnFe}_2\text{O}_4$  modified with (c) by *Ziziphus mauritiana* (d) *Salvadora persica*.

### 3.4 TEM analysis

The particle sizes of both pure and modified  $\text{ZnFe}_2\text{O}_4$  NPs were measured using TEM (Figures 4 (a) and (b)). The sizes of modified and unmodified photocatalyst were 7.59 nm and 5.95 nm for Pure  $\text{ZnFe}_2\text{O}_4$ ,  $\text{ZnFe}_2\text{O}_4$  by *Ziziphus mauritiana* and  $\text{ZnFe}_2\text{O}_4$  by *Salvadora persica* respectively. The morphologies of the nanoparticles in the images are spherical, indicative of organic compounds being present, which would have come from the plant extracts.

The results show that the agglomerations of NPs were excessed in all of the samples. This confirms that the residual organic compounds from the plant extracts were acting as capping ligands for the  $\text{ZnFe}_2\text{O}_4$  photocatalysts. Using plant extracts reduced the amount of agglomeration. Using *Salvadora persica* extract resulted in

small diameter particle sizes, which was expected when the capping method was used for ZnFe<sub>2</sub>O<sub>4</sub> synthesis.

Figures 4 (c) and (d) present the results of the <sup>4</sup> selected area electron diffraction (SAED) pattern. The SAED patterns reveal that the prepared materials are polycrystalline structures. The rings correspond to the crystal planes of (2 2 0), (3 1 1), (4 0 0) (5 1 1) and (4 4 0). As confirmed by analysing the XRD patterns, the prepared nanoparticles were crystalline.

The histograms plots shown in Figures 4 (e) and (f) depict the distribution of the size of the particles created, which was determined by analysing TEM images. Comparing the two histograms shows that the distribution of ZnFe<sub>2</sub>O<sub>4</sub> modified with *Ziziphus mauritiana* is narrower in scope than that of ZnFe<sub>2</sub>O<sub>4</sub> modified with *Salvadora persica*. The difference in the distribution of particle sizes might play a role in photodegradation performance.

Figure 4. Figure 4. TEM images of ZnFe<sub>2</sub>O<sub>4</sub> modified with (a) *Ziziphus mauritiana* (b) *Salvadora persica*. SAED images of ZnFe<sub>2</sub>O<sub>4</sub> modified with (c) *Ziziphus mauritiana* (d) *Salvadora persica*. Distribution of different particle sizes for ZnFe<sub>2</sub>O<sub>4</sub> modified by (e) *Ziziphus mauritiana* (f) *Salvadora persica*.

### **3.5 Optical properties analysis**

Figure 5 shows that, the prepared materials absorbed light radiation in the range of 480–850 nm, indicating they were active in sunlight. To calculate the band-gap energy the following equation was used:  $E_g \text{ (eV)} = 1240/\lambda$ , where,  $E_g$  is the band gap energy, and  $\lambda$  is the incident light wavelength (nm).

Figure 5. UV-vis absorption spectra of the  $\text{ZnFe}_2\text{O}_4$  nanoparticles modified with plant extracts.

Based on the results in figure 5, Tauc plots were used to estimate the value of band gap energies of the  $\text{ZnFe}_2\text{O}_4$  modified nanopartilces. The following equation was used:  $(Ah\nu)^n = B(h\nu - E_g)$  where,  $A$  is the light absorbance,  $h\nu$  is the photon energy,  $B$  is the constant related, and  $n$  can be  $\frac{1}{2}$  or  $2$  for direct or indirect transitions, respectively. Table 1 and Figure 6 show that the band gaps for  $\text{ZnFe}_2\text{O}_4$  modified with plant extracts are lower than the band gaps for pure  $\text{ZnFe}_2\text{O}_4$ . The band gaps were affected by doping  $\text{ZnO}$  with  $\text{Fe}$ ; the capping activity of the plant extracts might have reduced the band gap values and Fermi level was achieved due to the excitation of electrons was from valance band (VB) to conduction band (CB).

Figure 6. Plots of  $(Ah\nu)^n$  as a function of photon energy ( $h\nu$ ) of  $\text{ZnFe}_2\text{O}_4$  treated by plant extracts.

### ***3.6 Textural properties***

9  
The specific BET surface areas, pore volumes and pore diameters of the modified ZnFe<sub>2</sub>O<sub>4</sub> nanoparticles are presented in Table 2. The different extracts resulted in ZnFe<sub>2</sub>O<sub>4</sub> adopting different textural properties. Using the *Salvadora persica* extract gave the nanoparticles a significantly larger surface area than using the *Ziziphus mauritiana* extract. Figure 7 shows that the modified photocatalysts presented as mesoporous structures. The prepared biomaterials in this study are matched the fact of materials with greater surface area and pore volume have great numbers of active site located on the surfaces.

Figure 7. BET results of ZnFe<sub>2</sub>O<sub>4</sub> modified by plant extracts

### 3.7 Photocatalytic dye degradation studies

1  
In our previous study, the ability of ZnFe<sub>2</sub>O<sub>4</sub> nanoparticles to degrade CV dye in solution was compared against the abilities of CuFe<sub>2</sub>O<sub>4</sub>, CoFe<sub>2</sub>O<sub>4</sub> and NiFe<sub>2</sub>O<sub>4</sub> nanoparticles. The photocatalysts were prepared using the co-precipitation method; these were then calcined at temperatures ranging between 500°C and 900°C. Maximum catalytic performance was achieved when catalysts were calcined at 600°C. Consequently, for this study, ZnFe<sub>2</sub>O<sub>4</sub> was selected for modification with *Salvadora persica* and *Ziziphus mauritiana* extracts, and calcined at 600°C.

The ability of ZnFe<sub>2</sub>O<sub>4</sub> treated with to photodegrade CV dye under the visible light conditions was explored. The different plant extracts exhibited different

degradative abilities. The plant extracts affected the photocatalytic activity of the nanoparticles. In this instance, treating  $\text{ZnFe}_2\text{O}_4$  with *Ziziphus mauritiana* resulted in poorer elimination of CV dye compared to  $\text{ZnFe}_2\text{O}_4$  treated with *Salvadora persica*; the reaction and sunlight conditions were consistent for both samples.

Figure 8 (a) and (b) shows the comparative photocatalytic activity using 15 mg of modified  $\text{ZnFe}_2\text{O}_4$ . UV-vis spectra were obtained for blank controls and CV dye concentrations of 10 and 30 ppm in dark and sunlight conditions. No dye was degraded in the blank condition, but there was some degradation of dye in the darkness condition. The results are similar to those described previously.

The photocatalytic activities of the modified  $\text{ZnFe}_2\text{O}_4$  photocatalysts were improved by using neutral pH and sunlight. Two concentrations of CV dye (10 and 30 ppm) were loaded with 15 mg of plant extract-modified  $\text{ZnFe}_2\text{O}_4$  nanoparticles.  $\text{ZnFe}_2\text{O}_4$  with *Salvadora persica* extract achieved maximum photocatalytic degradation of 10 ppm of CV dye in 12 min. For pure  $\text{ZnFe}_2\text{O}_4$ , the maximum photocatalytic degradation of dye was reached in 30 min (Figures 8 (c) and (d)).

<sup>32</sup> This is consistent with earlier studies reported in the literature.

The photodegradative ability of *Salvadora persica* modified photocatalysts declined when the concentration of CV rose to 30 ppm. It reached maximum photodegradation within 25 min, which is longer than when the concentration of dye was 10 ppm. However, the performance of *Salvadora persica* modified photocatalysts was superior to the catalysts modified with *Ziziphus mauritiana* at the same concentration and exposed to the same conditions (Figures 8 (e) and (f)).

Several factors influence the photocatalytic degradation of dye in solution, including the duration of exposure, the concentration of the dye and the intensity of the sunlight.

This work shows that the type of plant extract used to modify the photocatalysts is also influential. Compared to  $\text{ZnFe}_2\text{O}_4$  modified with *Ziziphus mauritiana*, samples treated with *Salvadora persica* were more effective at degrading the dye. The plant extracts have several qualities, acting as stabilisers, reducing agents and the caps for the metals.

Figure 8. UV-vis spectra of photocatalytic degradation of (a) catalysts in darkness (b) blank (no catalyst) (c) *Salvadora persica*-modified  $\text{ZnFe}_2\text{O}_4$  in 10 ppm CV (d) Pure  $\text{ZnFe}_2\text{O}_4$  in 10 ppm CV (e) *Ziziphus mauritiana*-modified  $\text{ZnFe}_2\text{O}_4$  in 30 ppm CV dye (f) *Salvadora persica*-modified  $\text{ZnFe}_2\text{O}_4$  in 30 ppm CV.

### 3.8 Kinetics studies

This study explored the photocatalytic rate of  $\text{ZnFe}_2\text{O}_4$  modified with plant extract exposed to different concentrations of CV dye. The reactions followed pseudo-first-order kinetics and the initial decomposition reaction was calculated using the pseudo-first-order kinetic law.

$$-\ln C/C_o = k_{\text{app}}t$$



Where  $k_{app}$  is the rate constant of the pseudo-first-order reaction and  $t$  is the reaction time.

Table 2 presents the half-life and rate constant results. Compared to unmodified  $ZnFe_2O_4$ , modified nanoparticles displayed greater photodegradative ability, which is attributed to their morphological, structural and textural properties. Photocatalysts with high crystallite sizes and small particle sizes have fewer surfaced defects, which typically acts as recombination centres for the electron-hole pairs.

The dye concentration significantly affected the photocatalytic degradation reaction undertaken by the nanoparticles. Modified photocatalysts were able to degrade dye concentrations of 10 and 30 ppm in less time than unmodified photocatalysts.  $ZnFe_2O_4$  modified by *Salvadora persica* has smaller particle size with lower band gap and higher performance of photocatalytic degradation than  $ZnFe_2O_4$  modified by *Ziziphus mauritiana*. Materials with smaller particle sizes have lower band gap and the decreasing of band gap can be increased the oxygen vacancy and the energy level, which can be decreased recombination of  $\bar{e}$  and  $h^+$ . The results of  $C/C_0$  vs time and  $\ln(C/C_0)$  vs time plots are presented in figure 9.

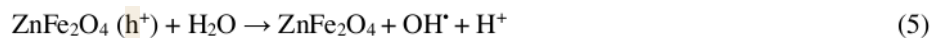
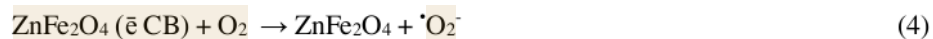
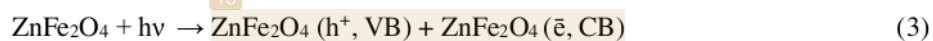
Figure 9.  $C/C_0$  vs time (left) and  $\ln(C/C_0)$  vs time (right) for pure and modified  $ZnFe_2O_4$  with a CV dye concentration of 10 ppm (top) and 30 ppm (bottom).

Table 2: Textural properties and kinetic studies of ZnFe<sub>2</sub>O<sub>4</sub> for the photodegradation of CV solutions

Photocatalysts	BET surface area (m <sup>2</sup> /g)	Pore Volume (cm <sup>3</sup> /g)	Pore Size (Å)	[CV] (ppm)	Degradation time (min)	k <sub>app</sub> (min <sup>-1</sup> )	t <sub>1/2</sub> (min)
ZnFe <sub>2</sub> O <sub>4</sub> + <i>Salvadora persica</i>	3.583	0.0317	533.53	10	12	0.65	1.07
				30	25	0.16	4.33
ZnFe <sub>2</sub> O <sub>4</sub> + <i>Ziziphus mauritiana</i>	0.965	0.0079	570.55	10	19	0.13	5.33
				30	30	0.10	6.93

### 3.9 Mechanism of photocatalytic degradation of CV dye

The proposed mechanisms by which modified ZnFe<sub>2</sub>O<sub>4</sub> nanoparticles photocatalytically degrades CV dye are as follows. First, CV dye adsorbs to the surface of the ZnFe<sub>2</sub>O<sub>4</sub> photocatalysts. When exposed to sunlight, the electrons (ē) in VB gets excited to the CB and hole ions (h<sup>+</sup>) was generate in the VB of the photocatalysts. Oxygen was reduced by electrons in the CB to become superoxide radicals (<sup>•</sup>O<sub>2</sub>). The h<sup>+</sup> attack the water molecules, releasing hydroxyl radicals (<sup>•</sup>OH). Radicals were attacked CV dye and degraded into CO<sub>2</sub> and H<sub>2</sub>O as equations 3-7 and figure 10 show.



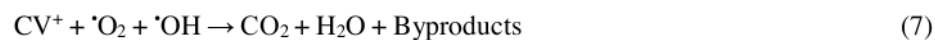


Figure 10. Schematic diagram of the photocatalytic degradation of CV solution over ZnFe<sub>2</sub>O<sub>4</sub> + *Salvadora persica* under sunlight irradiation

### 3.10 Reusability test

To evaluate the reusability of the ZnFe<sub>2</sub>O<sub>4</sub> photocatalysts created in this study, five iterations of recycling experiments were conducted under the same conditions. Figure 11 shows the decline in degradative ability of one set of photocatalysts after each cycle of use. After completing a reaction, the photocatalysts were retrieved, rinsed in distilled water and acetone, dried overnight in an oven set at 120° C and tested at the same conditions of fresh one. With each iteration, the photocatalytic degradation of CV dye declined, falling from 91% in the first cycle, to 85 % in the fifth cycle. This small decline reflects changes to the morphological, optical and textural properties of the photocatalysts. The results of the reusability experiments are similar to those reported by other researchers.

Figure 11. Percentage of decline in photodegradation of 30 ppm of CV dye exposed to recovered ZnFe<sub>2</sub>O<sub>4</sub> photocatalysts modified with *Salvadora persica* extract.

## 4 Conclusions

This study shows that modifying ZnFe<sub>2</sub>O<sub>4</sub> nanoparticles with *Salvadora persica* and *Ziziphus mauritiana* extracts creates nanoparticle products with superior ability to photodegrade CV dye solution in sunlight. The method used to synthesise the materials, their morphological, optical and textural properties and the reaction duration significantly influences the surface structure, optical properties, particle size and particle size distributions of ZnFe<sub>2</sub>O<sub>4</sub> treated with *Salvadora persica*. The photocatalyst was stable, being able to be used five times without experiencing marked decline in photocatalytic performance.

#### **Declaration of completing interest**

The author declares no conflicts of interest.

#### **Acknowledgment**

The author would like to thank the Deanship of Scientific Research, Albaha University, Saudi Arabia for the project fund (1442/29).

#### **Data availability statement**

Not applicable.

## ORIGINALITY REPORT

---

17%

SIMILARITY INDEX

12%

INTERNET SOURCES

11%

PUBLICATIONS

2%

STUDENT PAPERS

---

## PRIMARY SOURCES

---

- 1 Hossein Bayahia. " High activity of ZnFe O nanoparticles for photodegradation of crystal violet dye solution in the presence of sunlight ", Journal of Taibah University for Science, 2022  
Publication 2%
- 2 Hossein Bayahia. "Green synthesis of activated carbon doped tungsten trioxide photocatalysts using leaf of basil (Ocimum basilicum) for photocatalytic degradation of methylene blue under sunlight", Journal of Saudi Chemical Society, 2022  
Publication 2%
- 3 [sciencedocbox.com](https://www.sciencedocbox.com)  
Internet Source 1%
- 4 [dokumen.pub](https://www.dokumen.pub)  
Internet Source 1%
- 5 N. Matinise, K. Kaviyarasu, N. Mongwaketsi, S. Khamlich, L. Kotsedi, N. Mayedwa, M. Maaza. "Green synthesis of novel zinc iron oxide (ZnFe 2 O 4 ) nanocomposite via Moringa 1%

# Oleifera natural extract for electrochemical applications", Applied Surface Science, 2018

Publication

---

6	<a href="http://oaji.net">oaji.net</a> Internet Source	1 %
7	<a href="http://download.atlantis-press.com">download.atlantis-press.com</a> Internet Source	1 %
8	Submitted to Higher Education Commission Pakistan Student Paper	<1 %
9	<a href="http://coek.info">coek.info</a> Internet Source	<1 %
10	<a href="http://ijsrst.com">ijsrst.com</a> Internet Source	<1 %
11	<a href="http://www.orientjchem.org">www.orientjchem.org</a> Internet Source	<1 %
12	<a href="http://sciendo.com">sciendo.com</a> Internet Source	<1 %
13	<a href="http://repository.nwu.ac.za">repository.nwu.ac.za</a> Internet Source	<1 %
14	<a href="http://www.mdpi.com">www.mdpi.com</a> Internet Source	<1 %
15	<a href="http://www.scientiaricerca.com">www.scientiaricerca.com</a> Internet Source	<1 %

---

[res.mdpi.com](http://res.mdpi.com)

16

Internet Source

&lt;1 %

17

[jacobspublishers.com](http://jacobspublishers.com)

Internet Source

&lt;1 %

18

Mehrizadeh, Habib, Aligholi Niaei, Hui-Hsin Tseng, Dariush Salari, and Alireza Khataee. "Synthesis of ZnFe<sub>2</sub>O<sub>4</sub> nanoparticles for photocatalytic removal of toluene from gas phase in the annular reactor", Journal of Photochemistry and Photobiology A Chemistry, 2017.

Publication

&lt;1 %

19

[mdpi.com](http://mdpi.com)

Internet Source

&lt;1 %

20

[iaetsdjaras.org](http://iaetsdjaras.org)

Internet Source

&lt;1 %

21

[profdoc.um.ac.ir](http://profdoc.um.ac.ir)

Internet Source

&lt;1 %

22

[assets.researchsquare.com](http://assets.researchsquare.com)

Internet Source

&lt;1 %

23

[docplayer.net](http://docplayer.net)

Internet Source

&lt;1 %

24

[iopscience.iop.org](http://iopscience.iop.org)

Internet Source

&lt;1 %

25

[pubs.rsc.org](http://pubs.rsc.org)

Internet Source

<1 %

26

[www.shd.org.rs](http://www.shd.org.rs)

Internet Source

<1 %

27

[www.dovepress.com](http://www.dovepress.com)

Internet Source

<1 %

28

[www.jbcs.sbq.org.br](http://www.jbcs.sbq.org.br)

Internet Source

<1 %

29

Dhanalakshmi, B., K. Pratap, B. Parvatheeswara Rao, and P.S.V. Subba Rao. "Diffuse Dielectric Anomalies in  $(x).Bi_{0.95}Mn_{0.05}FeO_3-(1-x).Ni_{0.5}Zn_{0.5}Fe_2O_4$  multiferroic composites", *Journal of Magnetism and Magnetic Materials*, 2016.

Publication

<1 %

30

Fabbiyola, S., L. John Kennedy, T. Ratnaji, J. Judith Vijaya, Udaya Aruldoss, and M. Bououdina. "Effect of Fe-doping on the structural, optical and magnetic properties of ZnO nanostructures synthesised by co-precipitation method", *Ceramics International*, 2016.

Publication

<1 %

31

Moumita Mondal, Moupiya Ghosh, S.K. Pradhan. "Spectacular photocatalytic activity of mechanosynthesized heterostructured Bi-Fe-O nanocomposites in wastewater

<1 %



treatment containing colored and colorless pollutants", Journal of Molecular Liquids, 2021

Publication

32

[link.springer.com](https://link.springer.com)

Internet Source

<1 %

33

Xu, Qingqing, Jiantao Feng, Liangchao Li, Qiushi Xiao, and Jun Wang. "Hollow ZnFe<sub>2</sub>O<sub>4</sub>/TiO<sub>2</sub> composites: High-performance and recyclable visible-light photocatalyst", Journal of Alloys and Compounds, 2015.

Publication

<1 %

Exclude quotes Off

Exclude matches Off

Exclude bibliography Off